Chemical Engineering Journal 157 (2010) 530–538

Contents lists available at ScienceDirect

Chemical Engineering Journal

journal homepage: www.elsevier.com/locate/cej

Structured catalysts containing Co, Ba and K supported on modified natural sepiolite for the abatement of diesel exhaust pollutants

V.G. Milt[a], E.D. Banús[a], E.E. Miró[a,*], M. Yates[b], J.C. Martín[b], S.B. Rasmussen[b], P. Ávila[b]

[a] Instituto de Investigaciones en Catálisis y Petroquímica, INCAPE (FIQ, UNL – CONICET), Santiago del Estero 2829, 3000 Santa Fe, Argentina
[b] Instituto de Catálisis y Petroleoquímica, CSIC, C/Marie Curie 2, Cantoblanco, 28049 Madrid, Spain

ARTICLE INFO

Article history:
Received 27 October 2009
Received in revised form
30 December 2009
Accepted 31 December 2009

Keywords:
Diesel contaminants
Natural sepiolite
Soot combustion
NO_x adsorption

ABSTRACT

Natural sepiolite-supported catalysts, structured as highly porous ceramic discs were investigated for their application in diesel exhaust after treatment. Catalysts containing cobalt, potassium and barium, which are active ingredients for diesel soot combustion and NO_x adsorption, were prepared by wet impregnation of the support materials. The influence of incorporating CeO_2 as additive to the clay (sepiolite), along with activated carbon as pore generating agent (PGA) which is eliminated during the heat treatment step was studied. The additives affect the textural properties of the discs, that are related with their permeability and filtering capacity, but do not significantly alter their catalytic properties when Co and K are present as the active ingredients. The solids were characterised by several techniques: N_2 adsorption, mercury intrusion porosimetry (MIP), TGA-DTA, TPR, XRD and SEM. Different weight losses were observed as the temperature increased in TGA-DTA experiments owing to dehydrations and dehydroxylations of the sepiolite structure. The maximum rate of soot combustion for the Co- and K-containing catalyst was 366 and 453 °C for tight and loose contact, respectively. The bare sepiolite practically does not interact with $NO + O_2$, however, the addition of potassium and/or Ba caused a notable increase in the NO_x adsorption capacity. The catalytic activity results for the Co,K/sepiolite system and the excellent rheological properties of pastes that allow extrusion in various shapes which on heat treatment leads to conformed ceramic bodies with high mechanical strength, thermal resistance and large surface areas make this material an interesting potential candidate for the development of catalytic filters for diesel exhaust abatement applications.

1. Introduction

The main contaminants present in diesel emissions are soot particles and nitrogen oxides. Emissions of hydrocarbons and carbon monoxide are low and can be reduced still further with a diesel oxidation catalyst (DOC). However, depending solely on improvements in diesel engine design will not be enough to meet the requirements of future legislation for either soot or NO_x, making after treatment technologies the object of intense research [1].

An ambitious way to achieve diesel particulate removal is by the use of filters that support suitable catalysts which enables simultaneous soot filtration and combustion [2]. The idea of catalytic filters consists in the use of a catalyst able to regenerate the filter at temperatures comparable to those of diesel exhaust gases. NO_x absorbers (traps), combined with a reduction catalyst, constitute a relatively new control technology, which has been developed for both partial lean burn gasoline engines and diesel engines [3]. The absorbers, which are incorporated into the catalyst washcoat, chemically bind nitrogen oxides during lean engine operation. When the absorber capacity is saturated, the system is regenerated and released NO_x is catalytically reduced during a period of rich engine operation [4]. Since rich operation is not feasible in diesel engines periodic fuel injections are necessary.

Recently, soot oxidation in NO_x catalytic traps has been proposed as an alternative to simultaneously eliminate both NO_x and particle contaminants [5]. We have shown that, as the Co,Ba,K/CeO_2 catalyst pretreated with $NO + O_2$ (370 °C) was carefully mixed with soot (catalyst/soot = 20), soot combustion occurs even in the absence of gas phase oxygen due to the reaction between the soot particles and NO_x molecules originated by the decomposition of the trapped nitrate species [6]. The reaction between nitrate species and soot is the basis of the diesel particulate and NO_x reduction (DPNR Toyota system). Nitrates are formed in a catalytic trap composed of an alkali metal oxide after the NO to NO_x reaction takes place over Pt atoms. It is believed that surface nitrates are decomposed producing NO and very active O atoms, responsible for the soot oxidation [7,8].

Both catalytically active phases for NO_x and soot elimination and suitable materials for filter manufacture are subjects for intense research. In addition to high collection efficiency, the filter must

* Corresponding author. Tel.: +54 342 4536861; fax: +54 342 4536861.
E-mail address: emiro@fiq.unl.edu.ar (E.E. Miró).

1385-8947/$ – see front matter © 2010 Elsevier B.V. All rights reserved.
doi:10.1016/j.cej.2009.12.049

withstand the high temperatures of diesel exhaust gases (up to approximately 700 °C) and eventually, for short periods of time temperatures of over 975 °C [1]. The major trap types are: ceramic or metallic foams, ceramic or metallic yarns and wall-flow type monoliths [9]. The latter are formed from open (flow-through) monoliths into wall-flow type by plugging alternate channels at opposite ends of the monolith to force the incoming gases to pass through the porous walls.

Silver catalysts supported on modified sepiolite supports have recently been reported as efficient soot combustion catalysts [10]. Sepiolite is a natural hydrated magnesium silicate clay with the chemical composition ($Si_{12}Mg_8O_{30}(OH)_4(H_2O)_4{\cdot}8H_2O$) that has microporous channels of molecular dimensions within the fibres. The advantages of natural sepiolite as a catalytic support are the excellent rheological properties of pastes, produced using water as the lubricant, which allow extrusion in various shapes, that after heat treatment lead to conformed ceramic bodies with high mechanical strength, thermal resistance and surface areas [11]. With respect to diesel exhaust abatement, the porosity of this clay could play an important role in particulate trapping. Thus, this material is an interesting potential candidate for the development of catalytic filters for diesel exhaust abatement applications, having been successfully used by other groups for the development of monolithic catalysts for other environmental processes such as N_2O reduction [12].

The objective of this work was to study the use of sepiolite and modified sepiolite as supports of catalytically active phases for the abatement of diesel pollutants. Furthermore, the potential application of this material to manufacture catalytic filters was also examined. Structured supports in the shape of discs were prepared by extrusion in order to study the textural properties. Powder catalysts with similar compositions were prepared to investigate their performance as active phase supports. Catalytic experiments for both soot combustion and NO_x adsorption, together with characterisation of the structure and chemical properties of the solids were undertaken.

2. Experimental

2.1. Catalysts and structured supports preparation

Natural sepiolite (Tolsa S.A.), whose chemical composition (expressed as oxides) is: 60.8 wt.% SiO_2; 20.3 wt.% MgO; 4.6 wt.% Al_2O_3; 1.2 wt. % Fe_2O_3; 1.2 wt.% CaO; 1.1 wt.% K_2O and 0.4 wt.% Na_2O, was used to prepare structured catalysts as laminas that were subsequently cut as discs. These structured supports were made by extrusion of a paste prepared by kneading a mixture of sepiolite and an equal weight of activated carbon powder (AC, Chemviron) with water. The higher performance of sepiolite structured supports prepared with carbon as a pore generating agent (PGA) with respect to those without PGA has been recently demonstrated [13]. The PGA increases the porosity of the ceramic body due to its thermal degradation during the later heat treatment step.

Conformed supports were produced from extruding pastes with sepiolite and CeO_2, at a weight ratio of 65/35 with an equal weight of AC. The disc shaped materials were dried at room temperature for 48 h, then at 110 °C for 24 h and finally treated at 830 °C for 4 h to eliminate the PGA and form the stable ceramic. After heat treatment the discs were approximately 22 mm in diameter and 2 mm thick. The supports were designated as Sep and SepCe; indicating discs made from sepiolite with a 1/1 weight ratio sepiolite/PGA or 65/35/100 weight ratio for the sepiolite/CeO_2/PGA material. The active phases of Co, K or Ba were incorporated by impregnation of the conformed materials after calcination at 830 °C to remove the PGA and form the stabilised ceramic composite.

In order to perform soot combustion and NO_x adsorption experiments using conventional laboratory apparatus, powder catalysts were prepared by impregnation of either natural sepiolite or milled discs. Cobalt, potassium, cobalt–potassium and barium–potassium samples were prepared, employing solutions of Co(acetate)$_2$, KNO_3 and Ba(acetate)$_2$, so as to obtain the following weight percentages in the final catalysts: 5 wt.% K, 12 wt.% Co and 16 wt.% Ba. In the case of the bimetallic catalysts (Co–K and Ba–K) the precursor salts were simultaneously co-impregnated. After the impregnation procedure, the solids were calcined at 400 °C for 2 h in air. Some samples were also calcined for 2 h at 950 °C in order to study the effect of high temperatures on the structure of the catalysts.

2.2. Catalysts characterisation

2.2.1. Scanning electronic microscopy (SEM)

Morphologies were examined using a JEOL JSM-35C instrument, equipped with a secondary electron acquisition imaging system operated at 20 kV. Samples were added over the metallic sample holders using silver paint and were subsequently covered with gold by sputtering under an argon atmosphere.

2.2.2. X-ray diffraction (XRD)

The X-ray diffractograms were obtained with a Shimadzu XD-D1 instrument with monochromator using Cu Kα radiation in the continuous mode from $2\theta = 5$–80° at a scanning rate of 1°/min. The Shimadzu XD-D1 analysis software package was used for phase identification.

2.2.3. Nitrogen adsorption

The textural properties of the discs (specific surface areas (S_{BET}), micropore and mesopore volumes) were calculated from nitrogen adsorption at −196 °C determined on a Micromeritics Tristar apparatus. The samples were previously outgassed overnight at 300 °C ($P < 1.33 \times 10^{-2}$ Pa). The micropore volume was calculated from a *t*-plot analysis [14], taking the thickness of an adsorbed layer of nitrogen as 0.354 nm and assuming the arrangement of nitrogen molecules as hexagonal closed packed. The Harkins–Jura equation was chosen to relate the thickness of the adsorbed layer to the relative pressure since this employs a non-porous oxide to obtain the standard curve [15].

2.2.4. Mercury intrusion porosimetry (MIP)

A CE Instruments Pascal 140/240 apparatus was used to determine pore volume and neck size distributions over the range of 7.5 nm to 300 μm. The Washburn Equation [16] was used to analyse the pressure/volume data assuming a cylindrical non-intersecting pore model, taking the mercury contact angle and surface tension as 141° and 484 mN m^{-1}, respectively [15]. Samples were dried overnight at 150 °C previous to the measurement to ensure that they were free from any loosely bound adsorbed species.

2.2.5. Permeability (Ks)

According to Darcy's Law, $Q = KsA\Delta p/(L\eta)$, the permeability coefficient, *Ks*, was estimated from the variation of pressure drop generated by each material when a dry air flow passed through a calibrated area of a disc of the material with a constant thickness using a cell which is schematised in Fig. 1. A series of discs for each support were manufactured with different thicknesses and the experiments were carried out varying the total flow and measuring the pressure drop produced with each material at a constant cross-section area of 36.8 mm^2. The total flow was varied between 100 and 400 ml min^{-1}, and the thickness of the discs between 1.5 and 4 mm.

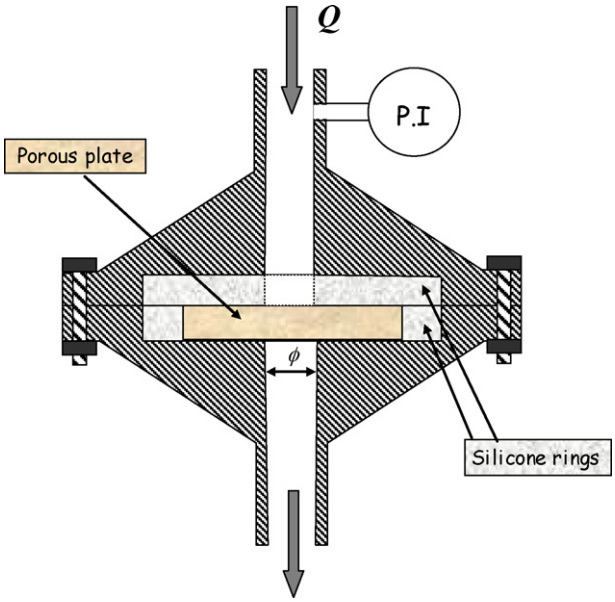

Fig. 1. Scheme of the cell used for permeability measurements.

2.2.6. Temperature-programmed reduction (TPR)

TPR experiments were performed in an Okhura TP-2002S system. The TPR runs were conducted using a heating rate of 10 °C/min in a flow of 5% H_2/Ar (45 ml/min) from room temperature up to 900 °C.

2.2.7. Catalytic soot combustion and NO_x adsorption

The soot was obtained by burning diesel fuel (Repsol – YPF, Argentina) in a glass vessel and subsequently collecting the soot from the vessel walls. Subsequently it was dried at 120 °C for 24 h before mixing with the powdered catalysts in an agate mortar for 3 min to obtain a tight contact or shaking the mixture in a pot to obtain a loose catalyst soot contact. In all cases, the weight ratio between the soot and the catalyst was 1/20.

The activity of the solids for the soot combustion was studied by TGA in a Mettler Toledo TGA/SDTA 851 equipment. Usually, 10 mg of mixes of catalyst + soot were heated from 25 to 700 °C at 10 °C/min in an air flow of 90 ml/min. TGA results are presented as w/w° (relative mass), being "w" the weight corresponding to any temperature T and "w°" the initial weight of the mixture soot + catalyst. In the case of the SDTA experiments, the information obtained from the equipment is (T_s–T_{ref}), where "T_s" and "T_{ref}" are the sample and the set temperatures, respectively.

The effect of the presence of 0.1% NO was studied by feeding O_2 (18%) + NO (0.1%) diluted in helium and carrying out the catalytic tests in a flow equipment. The exhaust gases were analysed with a Shimadzu GC-2014 chromatograph (with TCD detector), the CO concentration being negligible.

Micro-gravimetric experiments were performed in a Cahn 2000 equipment to study the interaction of the solid with NO + O_2. The sample was dried for 2 h at 400 °C in He and then stabilised at 70 °C, at which point the sample weight was determined (w°). Subsequently a mixture of NO (4%) + O_2 (18%) (He balance) was fed, until the sample was stabilised at 70 °C. After a constant weight was obtained the sample was heated to 490 °C at 5 °C/min; then maintained at this temperature for 10 min before cooling to 70 °C. The feed mixture was then changed to He and after stabilisation the sample was weighed. The heating program was subsequently repeated in He flow and the sample weighed at the end of this treatment at 70 °C.

3. Results and discussion

3.1. Textural properties of sepiolite-based discs

The fibrous nature of the sepiolite support may be observed in the SEM image shown in Fig. 2. The left picture (Fig. 2a) corresponds to the sepiolite sample, i.e., the solid mixed with activated carbon and calcined at 830 °C, where bundles of fibres of 0.1 μm × 1 μm are observed. A detail of a macropore (diameter about 2–2.5 μm) is shown in Fig. 2b, in addition to a soot aggregate scheme (usually soot aggregates are about 200–250 nm [17]). The size of the macropore shown in Fig. 2b is greater than those frequently found in sepiolite due to the addition of the PGA during the preparation of the material and subsequent decomposition when heated to 830 °C in air. As may be observed, soot aggregates can pass through sepiolite macropores but would be retained in the mesopores present among the bundles of fibres, which implies the potentiality of the system as a soot filter.

The nitrogen adsorption–desorption isotherms shown in Fig. 3 for sepiolite with and without CeO_2 correspond to type IIb [18], with hysteresis loops typical for materials with ill defined mesopores that extend into the macropore range, in accordance with the SEM results and with results observed by Blanco et al. [19] for Pt/sepiolite.

The total pore volume and pore size distribution of the conformed solids were determined by combination of the results from the corresponding nitrogen adsorption/desorption isotherms and MIP curves. In Table 1 the mesoporosity was calculated from the amount adsorbed at a relative pressure of 0.96 on the desorption branch, equivalent to the filling of all pores with a diameter below

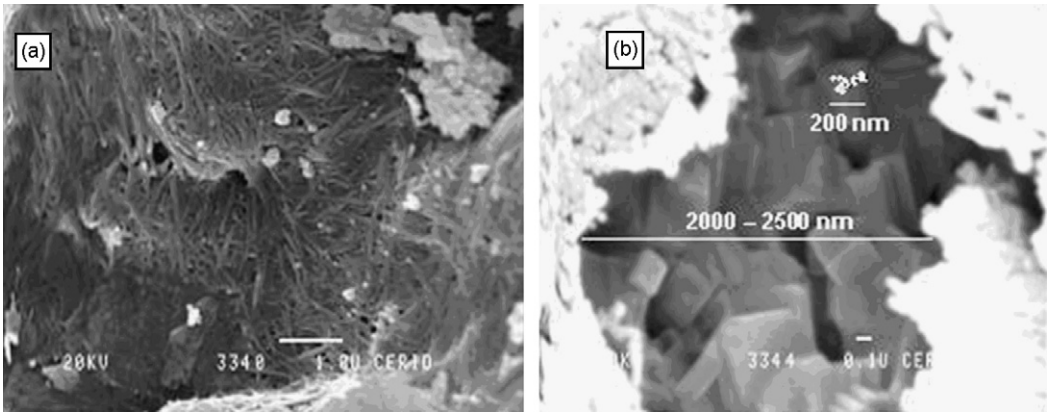

Fig. 2. SEM images of the Sep/PGA mixture calcined at 830 °C: (a) general view and (b) detail of a macropore, where a soot aggregate (size about 200 nm) is schematised.

Table 1
Textural properties of the supports.

Support	V_p ($cm^3\ g^{-1}$), meso[a,b], 2–50 nm	V_p ($cm^3\ g^{-1}$), macro[b], 50 nm to 10 μm	V_p ($cm^3\ g^{-1}$), Total[a,b]	THD (μm)	S_{BET} ($m^2\ g^{-1}$)	*Ks* (m^2)
Sep	0.30	0.12	0.42	0.08	53	–
Sep (PGA)	0.26	1.40	1.66	3.8	45	1.2
SepCe (PGA)	0.15	1.49	1.64	4.9	32	1.5

[a] As determined from N_2 adsorption experiments. No microporosity was observed.
[b] As determined from MIP experiments.

50 nm. The macroporosity was determined as the pore volume above 50 nm from the corresponding MIP curve. To combine the results from these two techniques, desorption data from the nitrogen isotherm was transformed into a diameter versus cumulative volume relationship by use of the Kelvin equation and correcting for the thickness of the adsorbed layer by employing the Harkins–Jura equation. In pore diameters above 50 nm the data obtained from the corresponding MIP curve was used. From these data, in Table 1 it may be seen that when CeO_2 was used as additive the specific surface area (S_{BET} = 32 $m^2\ g^{-1}$) was lower than for sepiolite (45 $m^2\ g^{-1}$). Since CeO_2 was added at a ratio of 65/35 by weight of sepiolite and oxide and taking into account that the PGA was burn out on heat treatment at 830 °C in air, then the specific surface area of the conformed materials after calcination would be due to the sum of the areas of the two remaining components if no reaction between the two had taken place. Thus, the 30% reduction in the specific surface area after CeO_2 incorporation was expected since ceria has a very low specific surface area. The corresponding *t*-plots for the materials calcined at 830 °C indicated that these supports did not possess micropores due to the folding of the sepiolite structure that occurs after the calcination at high temperature (330–600 °C).

The cumulative pore volume curves for the two supports after heat treatment at 830 °C obtained by combining the results from N_2 adsorption/desorption isotherms and MIP are presented in Fig. 4.

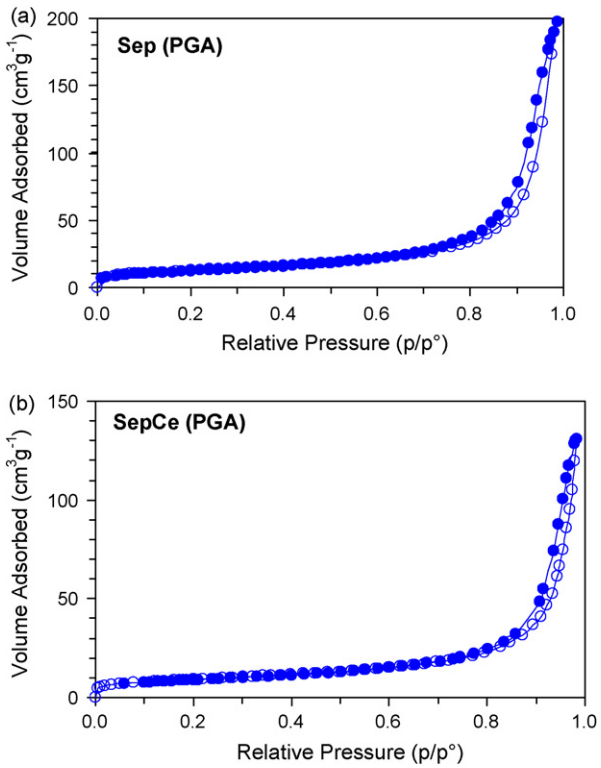

Fig. 3. Nitrogen adsorption–desorption isotherms for sepiolite supports without CeO_2 (a) and with CeO_2 (b).

For the material with Ce incorporated the reduction in the pore volume in pores of less than 200 nm, in accordance with the results obtained from the corresponding nitrogen isotherms (Fig. 3), indicated that this oxide was practically non-porous and the pore volume in this region was solely due to the sepiolite component. Above 200 nm the cumulative curves rose in accordance with the increased porosity created by the decomposition of the PGA, although the curve was displaced to wider pore diameters compared with the Sep/AC material (Fig. 4b).

The bimodal pore size distribution displayed by the materials after conformation and heat treatment is due to the mesopores within the bundles of sepiolite fibres, centred at about 40 nm, and the macropores centred at about 3 μm that are created during the combustion of the pore generating agent during heat treatment in air.

As described in Section 2, the permeability of these materials that are shown in Table 1, were determined by measuring the pressure drop generated when an air flow pass through a piece of each material with constant cross-section and thickness. From the data presented in Fig. 5 it may be observed that the inclusion of the CeO_2 in the support slightly increased the permeability of the material (*Ks* = 1.5) compared to that observed for the sepiolite sup-

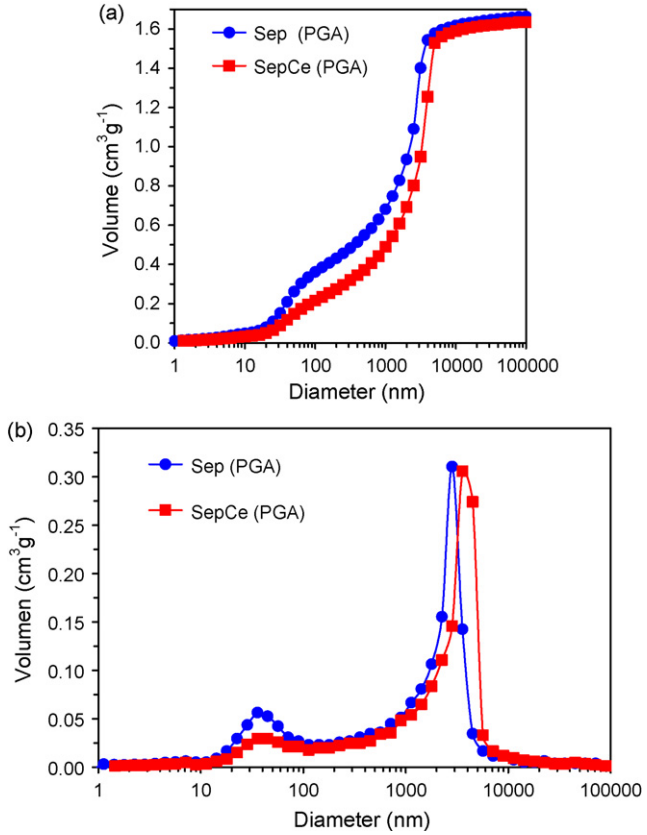

Fig. 4. Cumulative pore volumes (a) and pore size distribution (b) obtained by MIP + N_2 adsorption isotherms.

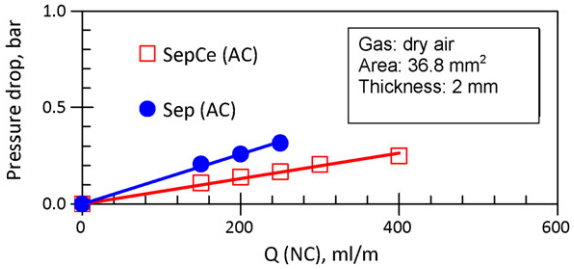

Fig. 5. Variation of the pressure drop obtained with supports, (●) Sep and (□) Sep-Ce as a function of the total flow for discs of 2 mm thickness. The total flow was varied between 100 and 400 ml min^{-1}. (For interpretation of the references to color in this figure caption, the reader is referred to the web version of the article.)

port (Ks = 1.2). This behaviour could be related to the differences observed in the porosities of these materials.

The transport of gas through the body of the discs made from these materials would be related to both the width of the widest through pores, indicated by the threshold diameters of the materials and the volume of these larger pores that reduce the tortuosity of the system. The threshold diameters (THD) from the corresponding MIP curves were: 3.8 and 4.9 μm, whereas the volumes of pores larger than 200 nm were: 1.23 and 1.36 $cm^3\ g^{-1}$ for Sep (PGA) and SepCe (PGA), respectively.

3.2. Thermal behaviour during calcination of discs

The DTA profiles between 200 and 950 °C, obtained on heating sepiolite and doped sepiolite in flowing air are shown in Fig. 6. For Sep, at approximately 90 °C the loss of hygroscopic water was observed ($Si_{12}Mg_8O_{30}(OH)_4(H_2O)_4{\cdot}8H_2O \rightarrow Si_{12}Mg_8O_{30}(OH)_4(H_2O)_4 + 8H_2O$). The endothermic peak at 295 °C corresponded to the first structural change, implying the loss of two of the four water molecules coordinated to magnesium ($Si_{12}Mg_8O_{30}(OH)_4(H_2O)_4 \rightarrow Si_{12}Mg_8O_{30}(OH)_4(H_2O)_2 + 2H_2O$) and the reversible folding of the structure. At 518 °C the loss of the other two water molecules occurs ($Si_{12}Mg_8O_{30}(OH)_4(H_2O)_2 \rightarrow Si_{12}Mg_8O_{30}(OH)_4 + 2H_2O$), leading to the irreversible folding of the structure. The signal observed at approximately 705 °C could be associated to the presence of calcite, a spurious material frequently found with natural sepiolite [20]. The well-defined signal observed at 830 °C corresponds to the loss of the constituent water of the structure by dehydroxylation with the subsequent formation of clinoenstatite ($Si_{12}Mg_8O_{30}(OH)_4 \rightarrow 8MgSiO_3 + 4SiO_2 + 2H_2O$), as reported in the literature [21–23]. The DTA curves for the impregnated sepiolite were qualitatively similar to that of the undoped solid.

In Fig. 7 the corresponding TGA curves are presented. These results, together with the different phase formations, will be further discussed in Section 3.3.

3.3. XRD characterisation

XRD diffraction patterns of the solids calcined at 400 °C are shown in Fig. 8. The natural sepiolite exhibited all the diffraction signals corresponding to this structure (2θ = 7.35; 13.32; 20.19; 26.73; 33.64; 37.57; 40.58; 47.76 and 62.70°) [24]. Peaks at 8.58 and 10.96° were also observed, which correspond to the sepiolite anhydride formed on calcination at 400 °C. Other signals observed in the diffractograms correspond to different oxides present in the natural sepiolite. When potassium was added to this structure, the crystallinity of the sepiolite appears enhanced. Signals corresponding to KNO_3 were also observed since this salt does not decompose until temperatures higher than 600–700 °C [25].

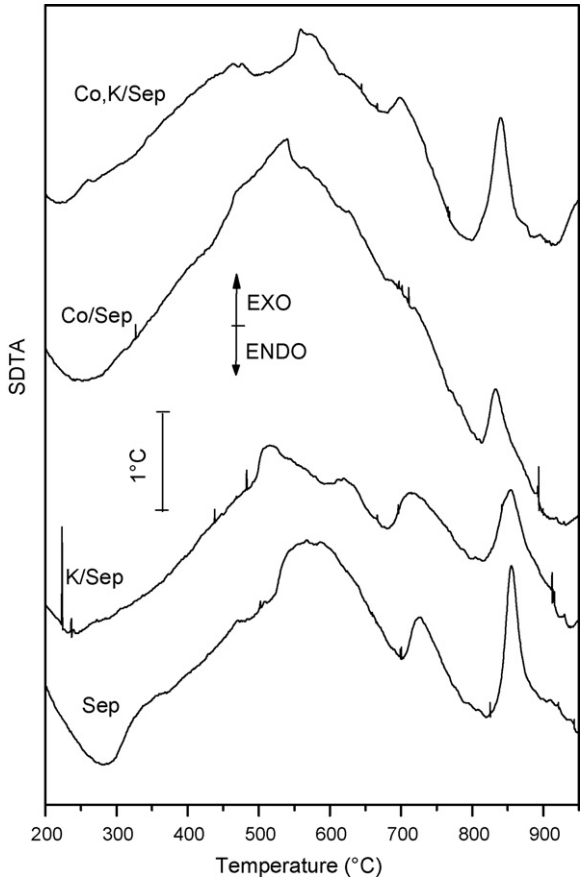

Fig. 6. Thermal behaviour (DTA) of pure and doped sepiolite. 10 mg of catalyst was heated from 25 to 700 °C at 10 °C/min in an air flow of 90 ml/min.

The sample containing Ba (Ba,K/Sep), prepared for NO_x adsorption experiments, was also examined by XRD. For this catalyst, peaks associated with $BaCO_3$ were observed; due to its thermal stability (decomposes at 1337 °C [26]). Barium carbonate was formed by the decomposition of Ba(acetate)$_2$. The signals corresponding to the sepiolite support were also observed in addition to KNO_3 peaks that appear together with the $BaCO_3$ peaks.

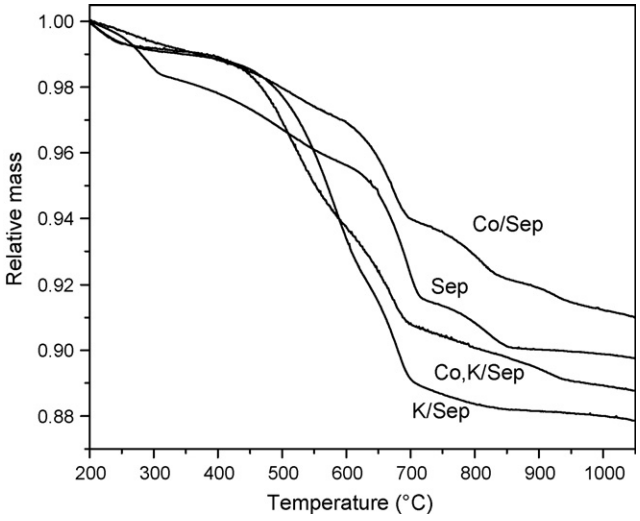

Fig. 7. Sepiolite-supported catalysts: TGA curves. 10 mg of catalyst was heated from 25 to 700 °C at 10 °C/min in an air flow of 90 ml/min.

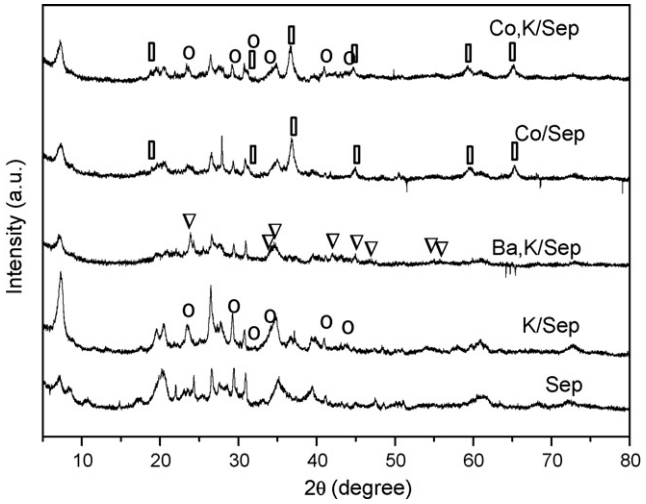

Fig. 8. Crystalline phases for the solids calcined at 400 °C (detected by XRD) (▯) Co_3O_4; (▽) $BaCO_3$; (◯) KNO_3.

Calcination at 400 °C of the cobalt doped sample (Co/Sep) gave rise to peaks corresponding to Co_3O_4, whereas when cobalt and potassium were incorporated (Co,K/Sep) after calcination at 400 °C peaks associated with both Co_3O_4 and KNO_3 were observed, in addition to the support signals.

The effect of a calcination temperature of 950 °C on the crystalline phases for the undoped and doped sepiolite is shown in Fig. 9. As expected, calcination of the sepiolite structure at temperatures higher than 800–830 °C provokes the complete dehydroxylation of the clay, leading to the formation of clinoenstatite ($MgSiO_3$) and SiO_2 [21,27]. However, in the K/Sep system a mixed crystalline oxide of magnesium and silicon, Mg_2SiO_4 (forsterite), was also formed. Comparing the diffractograms presented in Figs. 8 and 9 it may be observed that the higher calcination temperature caused decomposition of the KNO_3.

The diffractogram of the Ba,K/Sep system calcined at 950 °C shows the presence of both $MgSiO_3$ and Mg_2SiO_4 (although this latter mixed oxide appears in a lower relative proportion than in the case of the K/Sep solid) and $BaCO_3$.

When the Co/Sep solid was calcined at 950 °C, the signals of Co_3O_4 observed in the solid calcined at 400 °C disappear but the formation of another mixed oxide was observed: Co_2SiO_4, in addition to the presence of clinoenstatite and forsterite. In the case of the potassium-containing system (Co,K/Sep), the crystalline phases were the same as those observed in the undoped material, the only difference being the higher degree of crystallinity when the alkaline metal was present.

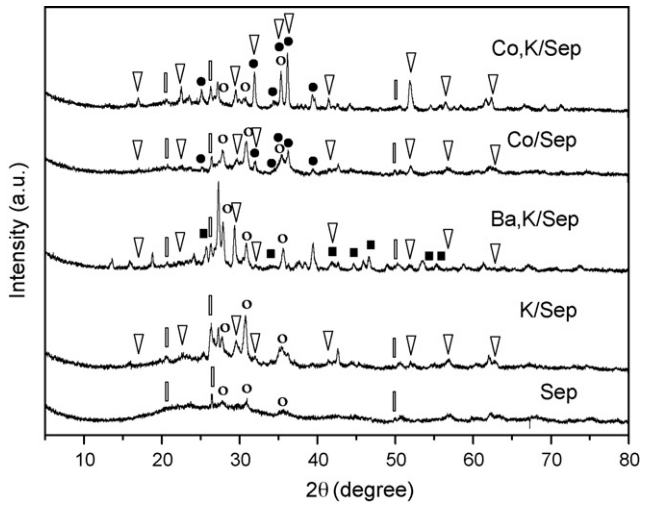

Fig. 9. Effect of the calcination temperature on the crystalline phases formed (solids calcined at 950 °C). (■) $BaCO_3$; (▽) Mg_2SiO_4; (●) Co_2SiO_4; (▯) SiO_2; (◯) $MgSiO_3$.

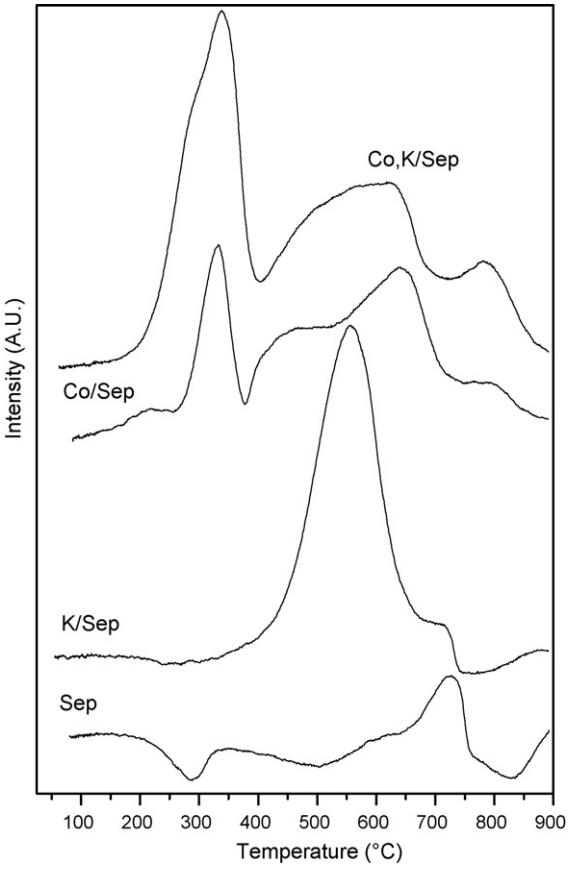

Fig. 10. Reducibility of the catalysts (solids calcined at 400 °C). TPR runs were conducted using a heating rate of 10 °C/min in a flow of 5% H_2/Ar (45 ml/min) up to 900 °C.

In general, two effects can be observed in samples containing potassium: the preferential formation of the forsterite phase (Mg_2SiO_4) in comparison with the formation of the clinoestatite mixed oxide ($MgSiO_3$), and the higher crystallinity of the samples. It has been suggested that, due to it low melting point, *K* improves the interaction between different phases thus increasing crystallinity and favoring the formation of mixed oxides. As a fact, similar effects have been observed in the case of Ba,Co mixed oxides, in which for the Ba,Co,O solid calcined at 1000 °C the presence of K induces both the development of the $BaCoO_{2.94}$ phase and the increase in crystallinity [6].

Considering the XRD results (Figs. 8 and 9) along with the TGA results described in the previous section (Fig. 7), the following aspects should be emphasized. There is a different behaviour for Co/Sep and Co,K/Sep when heating at temperatures higher than 400 °C. In both catalysts the $Si_{12}Mg_8O_{30}(OH)_4$ phase is formed at temperatures up to 500 °C, which was previously indicated as the irreversible folding of the sepiolite structure. However, the catalyst containing K (Co,K/Sep) exhibits an additional weight loss between 500 and 700 °C due to KNO_3 decomposition ($2KNO_3 \rightarrow K_2O + 2NO_2 + 1/2O_2$), and correspondingly, smaller weight values are observed in its TGA profile. At higher temperatures ($T > 700$ °C) the decomposition of the $Si_{12}Mg_8O_{30}(OH)_4$ phase begins. According to the XRD patterns, despite the fact that both clinoenstatite and forsterite are formed in Co/Sep and Co,K/Sep after

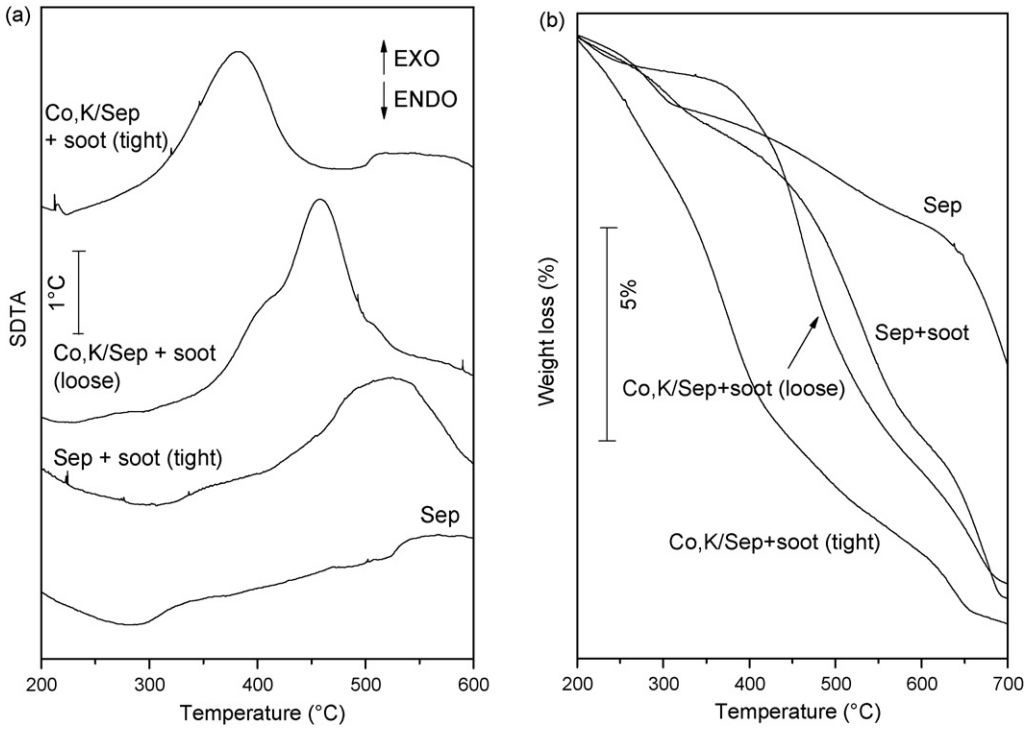

Fig. 11. Thermal evolutions when heating the bare sepiolite with or without soot and the catalytic effect of cobalt and potassium. SDTA experiments (a) and TGA experiments (b). 10 mg of mixes of catalyst + soot were heated from 25 to 700 °C at 10 °C/min in an air flow of 90 ml/min.

calcinations at 950 °C, $MgSiO_3$ is preferentially formed in Co/Sep and Mg_2SiO_4 in Co,K/Sep (Fig. 9). Nevertheless, the evolutions of both phases imply the same difference in weight (the same amount of water is lost in both cases):

$$Si_{12}Mg_8O_{30}(OH)_4(s) \rightarrow 8MgSiO_3(s) + 4SiO_2(s) + 2H_2O(g)$$

$$Si_{12}Mg_8O_{30}(OH)_4(s) \rightarrow 4Mg2SiO_4(s) + 8SiO_2(s) + 2H_2O(g)$$

On the other hand, cobalt silicate is formed by the reaction between cobalt and SiO_2 as follows: $2Co_3O_4(s) + 3SiO_2(s) \rightarrow 3Co_2SiO_4(s) + O_2(g)$, which implies a loss of oxygen and, consequently, an additional small decrease in weight. However, at high temperatures K_2O reacts with oxygen to give KO_2, which is the most thermodynamically stable potassium oxide. This is the reason for the lower decrease in weight for Co,K/Sep as compared with Co/Sep at temperatures higher than 700 °C. The same behaviour is observed when comparing K/Sep and the bare Sepiolite.

3.4. TPR results

TPR experiments were carried out to study the behaviour of the catalysts in the presence of a reducing mixture since catalytic activity for soot combustion is related to the oxidant capacity of the catalysts. The pure sepiolite (Fig. 10) displayed reduction peaks between 500 and 800 °C, probably due to the reduction of impurities present in the natural clay support. The K/Sep catalyst exhibited a reduction peak at 558 °C, which was probably related to the KNO_3 reduction. In the case of the Co/Sep catalyst, the low temperature reduction peak (maximum at 331 °C) corresponded to Co_3O_4 reduction. Nevertheless, the peaks that appear at higher temperatures could either correspond to the reduction of cobalt species retained in the sepiolite structure or to the reduction of mixed compounds formed by the reaction between cobalt and the other oxides in the sepiolite (as impurities). The Co,K/Sep TPR profile was similar to that observed for Co/Sep, where the wide peak between 390 and 700 °C was probably due to the reduction of KNO_3, together with Co species reduction, as in the case of Co/Sep.

3.5. Abatement of diesel exhaust pollutants: diesel soot combustion

TGA experiments with mixtures of soot and catalysts were performed, using both powdered sepiolite impregnated with active ingredients and calcined at 400 °C and milled discs. Although the thermal evolutions were different (the discs had been previously calcined at 830 °C thus the evolutions of sepiolite transformations were not present) the activity for soot combustion was unaffected. On bare sepiolite calcined at 400 °C soot burns with a maximum in the SDTA curve at 520 °C (Fig. 11a), although the broad signal also involves the sepiolite transformations. Two endothermic peaks at 295 and 518 °C when heating sepiolite in air corresponded to the reversible and irreversible folding of the sepiolite structure, respectively. Considering that non-catalytic combustion of soot takes place at ca. 600 °C, the undoped support exhibited some catalytic activity, probably related to the presence of impurities in the natural clay.

Fig. 11a also shows the SDTA curves for the Co,K/Sep catalyst mixed with soot both under tight and loose contact, with the corresponding TGA profiles shown in Fig. 11b. In the case of tight contact the maximum in the SDTA curve appeared at 366 °C and for loose contact at 453 °C, although this latter peak displayed two contributions, which would correspond to the burning of soot on sites of different types or could be associated with heterogeneity in the soot–catalyst mixture under loose contact. Although the TGA profiles were similar (Fig. 11b), they show some differences. A significant weight loss was observed at the beginning of the profile, i.e., at temperatures lower than 300 °C (>15 wt.%), which was consistent with the high water retention capacity of this solid. It should be pointed out that the expected weight loss due to the thermal decomposition of soot was 5 wt.%. Thus, the weight lost in the 200–700 °C range involved not only the combustion of soot

Table 2
Characteristic temperatures for soot burning.

Catalyst + soot	$T_{ignition}$ (°C)	T_{max} (°C)	T_{final} (°C)	Soot contact
Sepiolite	300	520	600	Tight
SepCe	296	481	608	Tight
Co/SepCe	289	461	590	Tight
K/SepCe	247	403	509	Tight
Co/Sep	254	454	585	Tight
	340	538	619	Loose
K/Sep	284	430	528	Tight
	352	523	582	Loose
Co,K/Sep	190	366	446	Tight
	301	453	589	Loose
Co,K/SepCe	236	360	445	Tight
	247	453	520	Loose

but also the multiple dehydrations of the clay support. In the case of the tight contact, the slope of the curve changed at ca. 400 °C, whereas for the loose contact, it takes place at ca. 500 °C, associated with two phenomena: ending of soot burning and support folding. At 600–700 °C the thermal decomposition of KNO_3 cause a weight loss observed in the TGA profiles, which was consistent with XRD patterns, where for the sample calcined at 400 °C the peaks corresponding to KNO_3 were observed but not for the sample calcined at 950 °C.

To the best of our knowledge the only previous reported work concerning the use of sepiolite as soot combustion catalyst supports is that of Güngör et al. [10], who reported that Ag/sepiolite catalysed soot oxidation with a temperature of maximum combustion rate of 500 °C. Our Co,K/Sep catalyst appears to enhance the catalytic properties of the sepiolite in a very effective way, reducing the temperature of maximum combustion rate by ca. 120 °C with respect to the reported catalyst.

Table 2 resumes the temperatures of maximum oxidation rate for the cobalt and/or potassium-containing catalysts either supported on the bare sepiolite or on the sepiolite that cointained CeO_2 as an additive (SepCe). Although CeO_2 is considered as an oxygen storage element, it seems to play no significant role in the studied systems, i.e., the activity of the solids was practically the same for both supports when Co and K were present as the active ingredients. Possibly, the heating of the support, with the corresponding folding of the structure, could produce an occlusion of the cerium in the support. An interesting effect of ceria could be the help in the the adjustment of specific surface, porosity and permeability, which are fundamental properties to be considered for the filter efficiency. The synergic effect of cobalt and potassium should be noted, where the oxidation activity, when both were present, was enhanced for both supports.

The presence of the NO in the reactor feed induces that the soot combustion rate maximum takes place at lower temperatures, both under loose and tight contact conditions (Fig. 12). The NO can react with O_2 giving NO_2 as a product. As it is well-known, the NO_2 oxidation capacity is higher than that of O_2. Moreover, this nitrogen oxide can be adsorbed on the surface as NO_x and act as a surface oxygen source for soot oxidation [6]. The effect of NO is more pronounced under loose contact conditions. Probably, under tight contact conditions dissociated oxygen is readily available at the catalyst surface.

3.6. Abatement of diesel exhaust pollutants: NO_x adsorption capacity

The interaction between the samples and $NO + O_2$ is shown in Fig. 13. The graph is divided into two parts, where the left corresponds to heating under $NO + O_2$ flow and the right to heating

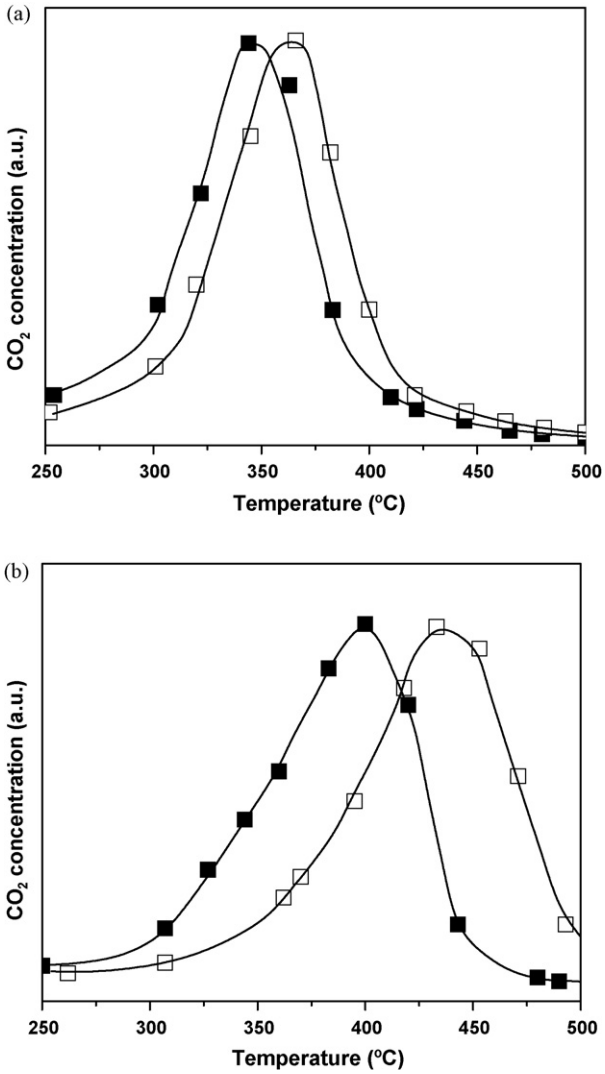

Fig. 12. Soot combustion: effect of NO (0.1%) in the gaseous feed. (a) Tight contact, (b) loose contact: (□) O_2 (20%); (■) O_2 (20%) + NO (0.1%). For other experimental conditions see Fig. 11.

under a helium stream. Neither the cooling under the oxidising atmosphere nor the cooling in helium is represented in the graph. The "*y*" axis shows the relative mass (w/w°), where "*w*" is the sample mass at any temperature (T) and w° is the mass at the beginning of the $NO + O_2$ treatment, i.e., after the helium pre-treatment up to 400 °C. When $w/w^\circ = 1$ means no interaction between the sample and NO_x (no NO_x adsorption) was observed.

The bare sepiolite practically does not interact with $NO + O_2$ (Fig. 13), however, the addition of potassium (K/Sep) caused a notable NO_x adsorption at 70 °C. When heating under $NO + O_2$, the weight did not change up to 200 °C but subsequently up to 490 °C it decreased. With cooling under NO_x the NO_x storage capacity observed at 70 °C at the beginning of the treatment was not recovered and heating under the inert atmosphere did not modify the weight. Although potassium was added to the catalyst as KNO_3 (salt saturated in NO_2 that does decompose below 490 °C as observed in the TGA experiments), the strong interaction between K/Sep and $NO + O_2$ at 70 °C would be associated to the strong basicity given by the KNO_3 alkaline salt. It should be noted that although natural sepiolite contained Na and K (see Section 2), in the prepared catalysts it was added in a much higher proportion (5 wt.%).

The system containing both barium and potassium (Ba,K/Sep) exhibited an even higher adsorption capacity of $NO + O_2$ at 70 °C

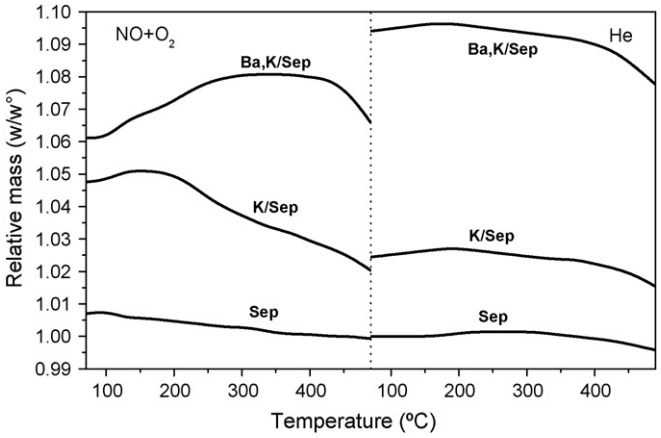

Fig. 13. NO_x adsorption for catalysts calcined at 400 °C, being "$w(T)$" the weight corresponding to any temperature T and w° that obtained after the He pre-treatment at 400 °C. For other conditions see Section 2.

than the system only containing potassium. Heating under $NO + O_2$ flow produces increasing weights up to 425 °C but above this temperature the weight decreased slightly. The adsorption increased when cooled in $NO + O_2$ and heating in helium diminished the weight very little. Thus, after the complete experiment in the microbalance the relative mass of the Ba,K/Sep catalysts was $\gg 1$, which implied a very good NO_x trapping capacity of this system. We have previously detected a similar behaviour for the Ba,K/CeO_2 system [6], although for the Ba,K-containing system supported on CeO_2 the decreasing tendency observed above 425 °C was not observed. This decrease in weight is not occasioned by a structural change of the sepiolite (Fig. 13), but could be associated to the presence of potassium (since the reaction between Ba and NO_2 to give barium nitrate is irreversible: $BaCO_3 + 2NO_2 + 1/2O_2 \rightarrow Ba(NO_3)_2 + CO_2$).

4. Conclusions

The catalytic activity results indicate that the Co,K/Sepiolite system demonstrated a good behaviour for diesel soot combustion. The support material (natural sepiolite) permitted easy extrusion so that the studied Co,K/Sepiolite system had a good potential for the preparation of catalytic filters for the elimination of particulate matter from diesel combustion. During soot combustion simultaneous transformations in the sepiolite structure, due fundamentally to the loss of water, took place. Sepiolite was chosen for the extrusion of pastes that on firing led to ceramic supports with controllable textural characteristics due to their excellent rheological properties. However, after firing at high temperature to decompose the PGA and gain mechanical strength the stable phases are clinoenstatite and forsterite. The use of PGA's is necessary in order to increase the porosity both in terms of pore volume and pore width. Wide macro-pores in the range of 10–50 μm are necessary to trap the soot particles without causing an excessive pressure drop when conformed as "wall-flow" monolithic structures.

Acknowledgements

The authors kindly thank the financial support received from ANPCyT (PICT No. 14-38391), the Universidad Nacional del Litoral (CAI+D programme) and from the Ministerio de Ciencia e Innovación (MICIN) CTM2008-06876-C02-02/TECNO. We also acknowledge the support received from CONICET (Argentine) and CSIC (Spain) (Resolution No. 2354/05).

References

[1] D. Fino, P. Fino, G. Saracco, V. Specchia, Chem. Eng. Sci. 58 (2003) 951.
[2] G. Saracco, C. Badini, V. Specchia, Chem. Eng. Sci. 54 (1999) 3035.
[3] A.W. Majewski, NOx adsorbers, in: Diesel Net Technology Guide, 2001, www.Diesel.Net.com.
[4] R.M. Heck, R.J. Farrauto, Appl. Catal. A: Gen. 221 (2001) 443.
[5] K. Krishna, M. Makkee, Catal. Today 114 (2006) 48.
[6] V.G. Milt, M.A. Ulla, Miró, Appl. Catal. B: Environ. 57 (2005) 13.
[7] K. Nakatani, S. Hirota, S. Takeshima, K. Itoh, T. Tanaka, SAE paper 2002-01-0957.
[8] K. Itoh, T. Tanaka, S. Hirota, T. Asanuma, K. Kimura, K. Nakatani, US patent, US6,594,911 (2003).
[9] D. Fino, Sci. Technol. Adv. Mater. 8 (2007) 93.
[10] N. Güngör, S. Işçi, E. Günister, W. Mišta, H. Teterycz, R. Klimkiewicz, Appl. Clay Sci. 32 (3–4) (2006) 291.
[11] J. Blanco, P. Avila, M. Yates, A. Bahamonde, Stud. Surf. Sci. Catal. 91 (1995) 755.
[12] S. Suárez, M. Yates, A.L. Petre, J.A. Martín, P. Ávila, J. Blanco, Appl. Catal. B: Environ. 64 (2006) 302.
[13] J. Blanco, A.L. Petre, M. Yates, M.P. Martín, S. Suarez, J.A. Martín, Adv. Mater. 18 (9) (2006) 1162.
[14] B.C. Lippens, J.H. de Boer, J. Catal. 4 (1965) 319.
[15] M. Yates, J. Blanco, M.A. Martin-Luengo, M.P. Martín, Micropor. Mesopor. Mater. 65 (2003) 219.
[16] E.W. Washburn, Proc. Nat. Acad. Sci. U.S.A. 7 (1921) 115.
[17] C. Van Gulijk, J.C.M. Marijnissen, M. Makkee, J.A. Moulijn, A. Schmidt-Ott, Aerosol Sci. 35 (2004) 633.
[18] F. Rouquerol, J. Rouquerol, K. Sing, Adsorption by Powders & Porous Solids Principles, Methodology and Applications, Academic Press, 1999.
[19] J. Blanco, A.L. Petre, M. Yates, M.P. Martín, J.A. Martín, M.A. Martín-Luengo, Appl. Catal. B: Environ. 73 (2007) 128.
[20] R. Ruiz, J.C. del Moral, C. Pesquera, I. Benito, F. González, Thermochim. Acta 279 (1996) 103.
[21] R.L. Frost, Z. Ding, Thermochim. Acta 397 (2003) 119.
[22] B.F. Jones, E. Galan, in: S.W. Bailey (Ed.), Sepiolite and Palygorskite: Hydrous Phyllosilicates, Reviews in Mineralogy, 19, Mineralogical Society of America, 1988, pp. 631–674, Chapter 16.
[23] H. Nagata, S. Shimoda, T. Sudo, Clays Clay Miner. 22 (1974) 285.
[24] M.R. Weir, E. Rutinduka, C. Detellier, C.Y. Feng, Q. Wang, T. Matsuura, R. Le Van Mao, J. Membr. Sci. 182 (2001) 41.
[25] V.G. Milt, C.A. Querini, E.E. Miró, Thermochim. Acta 404 (2003) 177.
[26] J.P. Breen, M. Marella, C. Pistarino, J.R.H. Ross, Catal. Lett. 80 (3–4) (2002) 123.
[27] M. Molina-Sabio, F. Caturla, F. Rodríguez-Reinoso, G.V. Kharitonova, Micropor. Mesopor. Mater. 47 (2001) 389.